Provided for non-commercial research and education use.
Not for reproduction, distribution or commercial use.

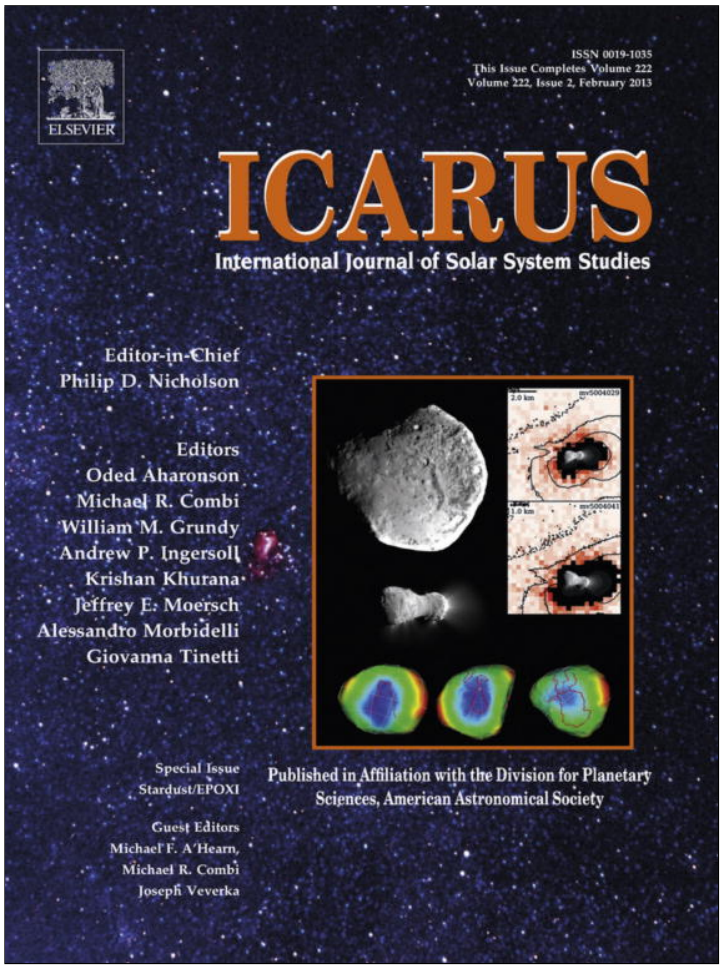

This article appeared in a journal published by Elsevier. The attached copy is furnished to the author for internal non-commercial research and education use, including for instruction at the authors institution and sharing with colleagues.

Other uses, including reproduction and distribution, or selling or licensing copies, or posting to personal, institutional or third party websites are prohibited.

In most cases authors are permitted to post their version of the article (e.g. in Word or Tex form) to their personal website or institutional repository. Authors requiring further information regarding Elsevier's archiving and manuscript policies are encouraged to visit:

http://www.elsevier.com/copyright

Author's personal copy

Icarus 222 (2013) 786–798

Contents lists available at SciVerse ScienceDirect

Icarus

journal homepage: www.elsevier.com/locate/icarus

Photometry and imaging of Comet 103P/Hartley in the 2010–2011 apparition

Giannantonio Milani [a,b,s,*], Erik Bryssinck [c,a], Martino Nicolini [d,a], Herman Mikuž [e,a], Giovanni Sostero [f,a], Paolo Bacci [g,a], Walter Borghini [h,a], Dario Castellano [a], Mauro Facchini [d,a], Giancarlo Favero [i,a], Gianni Galli [j,a], Ernesto Guido [f,a], Bernhard Hausler [k,a], Kamil Hornoch [l,a], Nick Howes [m,n,a], Rolando Ligustri [o,a], Carmen Perrella [a], Enrico Prosperi [p,a], Jure Skvarč [e,a], Jiří Srba [q,a], Roberto Trabatti [r,a], Carlo Vinante [s,a], Gyula Szabó [t,a]

[a] CARA Project, Astrofili Italiani, IASF INAF via Fosso del Cavaliere 100, 00133 Roma, Italy
[b] Dipartimento di Scienze Biomediche, Università di Padova, viale G. Colombo 3, 35131 Padova, Italy
[c] BRIXIIS Observatory, Eyckensbeekstraat, 9150 Kruibeke, Belgium
[d] G. Montanari Observatory, via Concordia 200, 41032 Cavezzo, Italy
[e] Črni Vrh Observatory, 5274 Črni Vrh nad Idrijo, Slovenia
[f] Remanzacco Observatory (AFAM), via S. Stefano, 33047 Remanzacco, Italy
[g] Centro Astronomico Libbiano, Loc. via della Chiesa 32, 56037 Peccioli, PI, Italy
[h] Osservatorio Astronomico Naturalistico di Casasco, Strada Ca'Simone, 15050 Casasco, Italy
[i] Celado Observatory, UATV via Venezia 18, 38053 Castello Tesino, Italy
[j] GiaGa Observatory, Via Mozart 4, 20010 Pogliano Milanese, MI, Italy
[k] Maidbronn Observatory, Albin-Joerg Str., D 97222 Maidbronn, Germany
[l] Astronomical Institute, Academy of Sciences of the Czech Republic, Fričova 1, CZ-25165 Ondřejov, Czech Republic
[m] LCOGT/Faulkes Telescope North, Haleakala High Altitude Observatory Site, 96768 Maui, HI, United States
[n] Cherhill Observatory, White Horse View, Cherhill, Wiltshire, United Kingdom
[o] Talmassons Observatory (C.A.S.T.), via Cadorna, 33030 Talmassons, Italy
[p] Castelmartini Observatory, via Bartolini 1357, 51036 Larciano, Italy
[q] Observatory Valašské Meziříčí, Vsetínská 78, CZ-75701 Valašské Meziříčí, Czech Republic
[r] Stazione Astronomica Descartes, via Lambrinia 4, 27013 Chignolo Po', Italy
[s] Associazione Astronomica Euganea, via Tommaseo, 35131 Padova, Italy
[t] Konkoly Observatory of the Hungarian Academy of Sciences, P.O. Box 67, 1525 Budapest, Hungary

ARTICLE INFO

Article history:
Available online 21 September 2012

Keywords:
Comets, dust
Photometry
Comets, dynamics

ABSTRACT

The results of a CARA (Cometary Archive for $Af\rho$) campaign on Comet 103P/Hartley 2 are presented. The main goal was to monitor extensively the comet during the apparition with CCD R and I imaging and photometry, as a support of EPOXI mission.

The $Af\rho$ quantity showed a progressively rising ascending branch, followed by an apparent flat maximum that lasted for 2 months, from about −10 to +50 days from perihelion. In this period, $Af\rho$ peaked at around 100 cm in R band with strong short term fluctuations between 70 and 140 cm. Early signs of activity were detectable well before perihelion (about 80–90 days before) and a random variability is also present in the descending branch after perihelion. Three post perihelion data points (between +55 and +61 days) from the 1997–1998 apparition show a bit higher $Af\rho$ value of our observation and a similar fast variation.

The average $Af\rho$ behavior, corrected for the solar phase effect, is strongly asymmetric and shows a more steeper ascending branch, approaching to perihelion.

Morphology and coma asymmetry, as well as the sunward and tailward profiles are examined. An average gradient indicatively between $\sim\rho^{-0.7}$ and ρ^{-1} is observed in the inner coma ($\rho < 2000$ km). Ten small amplitude outbursts have been detected and two ones were suspected.

© 2012 Elsevier Inc. All rights reserved.

* Corresponding author at: Dipartimento di Scienze Biomediche, Università di Padova, viale G. Colombo 3, 35131 Padova, Italy. Fax: +39 49 8276048.
E-mail addresses: milani@mail.bio.unipd.it, milani.giannantonio@tiscali.it (G. Milani).

0019-1035/$ - see front matter © 2012 Elsevier Inc. All rights reserved.
http://dx.doi.org/10.1016/j.icarus.2012.09.004

Author's personal copy

1. Introduction

Comet 103P/Hartley was discovered in 1986 by Malcom Hartley (IAU Circ. 4015). It is a Jupiter Family comet that was perturbed by Jupiter and moved to an orbit with a perihelion distance of 1.05 AU, becoming an interesting candidate for space missions. It was selected in 2007 as the target of EPOXI mission, that is the extension of the successful Deep Impact Mission, targeting Comet 9P/Tempel (A'Hearn et al., 2005). The spacecraft flyby was planned for early November 2010 and an Earth and space-based campaign started in 2008 to complement the space mission (Snodgrass et al., 2010; Meech et al., 2011; Lisse et al., 2009). The successful results from EPOXI mission and from the correlated observing campaigns, e.g. the detection of a water isotopic composition similar to that of the Earth oceans (Hartogh et al., 2011), gave an exciting insight to this particular comet.

The CARA project (Cometary Archive for Amateur Astronomers, renamed now as Cometary Archive for $Af\rho$), already contributed to support the Deep Impact Mission with a specific photometric ground-based campaign (Milani et al., 2007). Similarly to this, we organized the 103P/Hartley campaign with the participation of many skilled amateur astronomers worldwide.

The goal was mainly to perform a photometric survey, collecting $Af\rho$ data (A' Hearn et al., 1984) that allows a monitoring of the dust cross section during the apparition. The comet was observed during 11 months, while we have assigned an extensive importance to the days of the encounter.

For the survey we made use of small size telescopes with apertures typically between 20 and 80 cm, which was integrated by data from the 2 m Faulkes Telescope North around flyby.

The observing campaign has uncovered a quite complex behavior of Comet Hartley-2, characterized by periods of short term variability, particularly around perihelion.

2. Observations

The 103P/Hartley observing campaign was planned using with the same observing and reduction procedures as for Comet 9P/Tempel 1 (Milani et al., 2007), and applied also for 67P/Churyumov–Gerasimenko (Fulle et al., 2004, 2010). Some improvements have been done in respect to the early CARA approach (Szabó et al., 2010) introducing routinely a much larger number of multi-aperture measurements in photometry and paying more attention to the selection of the reference stars as close as possible to the solar color (Hardorph, 1978). Some reference stars have been extracted also from the SuperCosmos Sky Survey (Hambly et al., 2001). Data from images affected by problems alerting for a mediocre measurement, e.g. a non-negligible sky gradient, comet superimposed to bright stars, insufficient low S/N, have been rejected from the analysis.

CCD images were taken in R and I Cousins filters (Bessel, 1990), and one narrowband filter (647 nm 10 nm FWHM) (Fulle et al., 1997). To fulfill the requirements of photometry, dark and bias subtraction and flat field correction were performed. Furthermore, if it was ever possible, the comet field was adjusted in such way that there was at least one reliable reference star in the image. Alternatively, reference stars were selected in nearby fields, as close as possible to the comet (within 3°). Routinely, a sequence of more images has been averaged to improve the signal to noise ratio. As an example, a typical sequence of 10 images, each with a 1 min exposure time, and with a 30 cm diameter telescope gave a final signal-to-noise ratio around 100 for a 9–10 magnitude object.

The $Af\rho$ quantity was calculated from a multi-aperture photometry of the comet, usually obtained with a 2 pixels increment in the window size. The lower limit of the window was 3 pixel in most cases, while the upper limit is set up by the observer in order to frame, if possible, all the coma or the part of it that is not affected by bright stars contamination. The size (radius) of the windows is then converted to kilometers at the comet. To standardize the data the $Af\rho$ quantity was then interpolated (linear interpolation) to a constant 5000 km radius aperture.

The reference star was measured in a single aperture that was 4–5 times larger than the stellar FWHM. Differential photometry was applied to measure the apparent brightness of the comet, that was finally converted to flux ratio via the absolute brightness of the Sun.

Similarly to our experiences in the 9P/Tempel 1 campaign (Milani et al., 2007), the final photometric accuracy is mostly determined by the accuracy of the photometry of reference stars in the literature. Also, $Af\rho$ quantity is very sensitive to the biased estimate of the background (e.g. in crowded star fields or with gradients due to twilight, faint background nebulosity or light pollution), and is also sensitive to the flat field correction. The external estimated error, comparing different measurements from various sites and close to each other in time, is around 20–30% when the comet was farther and fainter, while the photometric accuracy rose to 10% around perihelion.

Three R band images from the 1997–1998 apparition (taken between +55 and +61 days after perihelion) were measured to compare the activity in two different apparitions.

The collected images were also useful to monitor the coma morphology in general.

3. Observational circumstances

The 2010–2011 apparition was favorable for the coordinated Earth based observing campaigns, because the comet passed close to Earth (around 0.1 AU) in late October–early November, allowing us to perform high spatial resolution observations of the perihelion passage. Due to the low inclination (13.6°) (Nakano and Green, 2009, 2011), the comet was always in favorable position in the sky allowing follow-up lasting for nearly one year.

The long observing window sampled a noticeable range of geocentric distance (Δ). The resolution of our images spanned indicatively from about 1500 km/arcsec to 100 km/arcsec during the campaign. Small instruments could attain an enough fine resolution only in a limited part of the apparition. But the image scale, about 2–3 arcsec/pixel in average, was always enough to get a homogeneous dataset. The seeing has also limited the resolution, that ranged from 1 arcsec (Faulkes Telescope North) to 4 arcsec (sites in suburban areas).

During our observing campaign the solar phase angle α varied between 20° and 60° introducing some bias in the analysis of the average brightening/fading rate as well in the peak value observed at perihelion Schleicher (2007) and Schleicher et al. (1998). To remove these unwanted effects and perform a normalization for a zero phase angle the photometric data have been corrected according to the discrete tabulated phase function data provided by Schleicher (Schleicher and Bair, 2011).

For the phase correction on $Af\rho$ we adopted the relation:

$$Af\rho\ (0) = Af\rho\ 1/(\mathrm{A} + \mathrm{B1}\alpha + \mathrm{B2}\alpha^2 + \mathrm{B3}\alpha^3 + \mathrm{B4}\alpha^4) \quad (1)$$

With:

$$\mathrm{A} = 1.01254 \pm 0.00932$$

$$\mathrm{B1} = -0.04102 \pm 0.00104$$

$$\mathrm{B2} = 0.00104 \pm 4.17224\mathrm{E}-5$$

$$\mathrm{B3} = -1.35788\mathrm{E}-5 \pm 7.17486\mathrm{E}-7$$

Author's personal copy

$$B4 = 7.52341E-8 \pm 4.47506E-9$$

$$(r = 0.9999\ SD = 3.82E-4)$$

where r is the correlation coefficient, SD is the standard deviation, α is the solar phase angle, $Af\rho$ is the observed value and $Af\rho$ (0) is the rescaled value for zero solar phase angle. The formula have been interpolated starting from the Schleicher discrete data for 20 deg < α < 60 deg. The bias introduced by the use of the polynomial model is negligible at our level of accuracy. A check has shown that the difference between the calculated and original Schleicher's data is smaller than 0.8%.

4. Data analysis

103P/Hartley 2 had been known as a relatively active and gas rich comet (Grosussin et al., 2004; Crovisier et al., 2004; Colangeli et al., 1999), with gas emissions in the visible part of the spectrum that could contaminate the wide R and I pass-bands. This was also confirmed by some V band images collected in December 1997 and January 1998 at the Črni Vrh Observatory (Slovenia), showing a relatively active comet with a well developed coma and a ion tail close to perihelion (Fig. 1) (other R band Črni Vrh Observatory images of the same apparition will be discussed later).

The R and I passbands usually are affected by weak gas emissions (Szabó et al., 2002), but for very active comets some degree of gas contamination is still expected. We found that the gas contamination in the $Af\rho$ quantity can be as high as 50% (a value measured for 157P/Ikeya Zhang), but in many other comets, it remains negligible. For Comet 103P/Hartley 2 (September 10, R = 1.24 AU, 47 days before perihelion) we obtained one narrowband measurement with the 647 nm/10 nm FWHM filter. This filter allows to measure the continuum away from any emission line. The narrow-band $Af\rho$ value (39 cm) is in good agreement with R wideband data (42 cm and 40 cm) obtained about 8–10 h before and after. This suggests that the gas contamination was smaller than our average estimated error. We also checked that our data was in good agreement with narrowband photometry by Lara et al. (2011), which confirms the negligible gas contamination in our wide-band photometry.

We also experienced a systematic difference between I and R data: I band $Af\rho$ is, on average, approximately 10% higher than in R band. This difference is similar to what is observed for other comets (e.g. 78P/Gehrels, 9P/Tempel 1), very close, or even below, our average observational error. In this analysis I band data have been rescaled to be comparable with R ones adopting the relation

$$R_{(I)} = 0.9I \quad (2)$$

where $R_{(I)}$ is the I value rescaled to R.

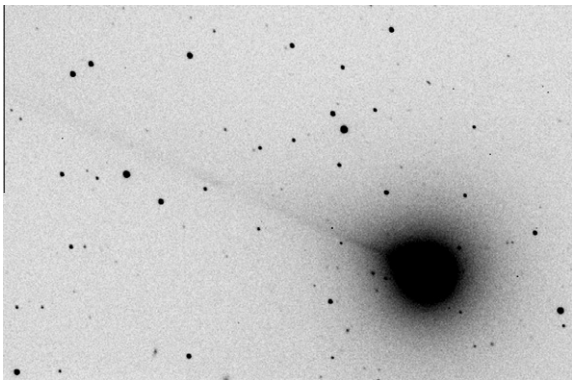

Fig. 1. Periodic Comet 103P/Hartley 2 observed at the Črni Vrh Observatory (Slovenia) on 1997 December 28.727UT with the 36-cm f/6.7 Schmidt–Cassegrain telescope V filter and CCD. Exposure time was 5 min.

Table 1
Contributing observers and observing sites.

Name	Observatory	Country	Image scale (arcsec/pixel)	Filter	Observer code
Bryssinck E.	Brixiis (Kruibeke)	Belgium	0.9–1.0	R.I	BRY01
Bryssinck E.	Tzec Maun obs.	USA	0.9– 1.0	R	
Bacci P.	Libbiano	Italy	3.20–3.82	R	BAC01
Borghini W.	Casasco	Italy	2.40–3.05	R	BOR01
Favero G.	Celado obs.	Italy	2.0	R	CELA1
Galli G.	Private obs. Milan	Italy	3.00–3.62	R	GAL01
GuidoE. Sostero G.	Remanzacco	Italy	2.40–3.05	R	AFAM1
GuidoE. Sostero G.	GRAS. Mayhill	USA		R	
GuidoE. Sostero G.	Tzec Maun obs.	USA		R	
Hausler B.	Maidbronn	Germany		R.I	HAU01
Howes N.	Faulkes North	U.K.	0.28	R	FAUL1
Ligustri R.	Talmassons	Italy	3.20–3.82	R.S	LIG01
Mikuž H.	Črni Vrh	Slovenia	2.40–3.04	R	CRNI1
Milani G.	Private obs. Padova	Italy	2.3	R.I	MIL01
Nicolini M.	Cavezzo	Italy	2.40–3.04	R	NIC01
Prosperi E.	Castelmartini	Italy	2.98–3.62	R	PRO01
Skvarč J.	Črni Vrh	Slovenia	2.0	R	CRNI1
Hornoch K.	Ondřejov	Czech Republic	1.05	R	HOR01

Due to the fast variability of the comet the calculation of the R–I color index was possible only for few data that include simultaneous R and I observations. We found R–I = 0.35 ± 0.12 and 0.44 ± 0.18 respectively on August 4.96 and December 10.99. It is close to solar color (R–I = 0.33).

Sixteen observers joined the CARA observing campaign (Table 1) and were selected from 187 observing runs between 2010 June 15 and 2011 April 28, spanning from 134 days before the perihelion passage to 182 after. This made possible a long term homogeneous monitoring of the apparition.

5. Discussion

The photometric behavior of Comet 103P/Hartley during the 2010–2011 apparition, expressed by means of the observed $Af\rho$ quantity (in cm), is shown in Fig. 2. As already mentioned the data have been normalized (interpolated) to a 5000 km radius aperture at the comet and refer to R photometric band. $Af\rho$ data, not corrected for the solar phase effect, are reported in Table 2.

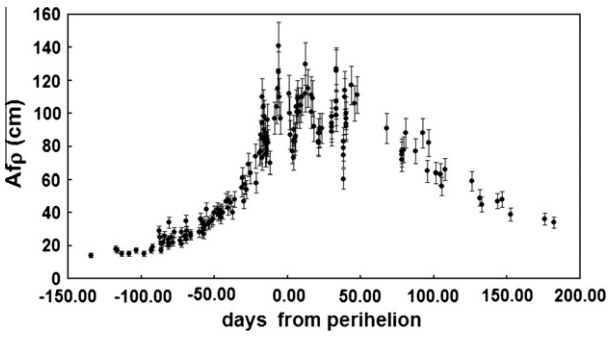

Fig. 2. Evolution of $Af\rho$ quantity (cm) of Comet 103P/Hartley 2 during the 2010/2011 apparition. The $Af\rho$ quantity refers to R and I (Cousins) photometry normalized to a standard 5000 km radius measuring window at the comet. I band data have been rescaled to match the R band data and are not corrected for the solar phase angle.

Author's personal copy

Table 2
Afρ data referred to a 5000 km radius measuring window at the comet.

Days from T	Julian Date	R (A.U.)	Δ (A.U.)	Phase angle	Phot. band	*Afρ* (cm)	err	Observer
-134.27	2455363.491	1.373	1.977	28.71	R	14	4	HOR01
-117.21	2455380.553	1.096	1.825	29.01	R	18	4	HOR01
-116.21	2455381.553	1.080	1.816	29.01	R	17	4	HOR01
-113.33	2455384.434	1.037	1.790	29.02	R	15	3	HOR01
-108.26	2455389.495	0.963	1.746	29.00	R	15	3	CRNI1
-103.38	2455394.384	0.895	1.702	29.01	R	17	4	HOR01
-97.83	2455399.927	0.821	1.653	29.02	Ru	15	3	AFAM1
-93.19	2455404.566	0.762	1.611	29.10	R	17	4	HOR01
-92.18	2455405.579	0.750	1.603	29.12	R	19	4	HOR01
-87.92	2455409.844	0.699	1.565	29.24	R	29	4	BRY01
-87.28	2455410.480	0.691	1.560	29.27	R	25	4	LIG01
-86.38	2455411.384	0.681	1.552	29.30	R	17	4	CRNI1
-86.37	2455411.385	0.681	1.552	29.31	R	21	4	LIG01
-86.34	2455411.417	0.680	1.552	29.32	R	21	4	AFAM1
-85.02	2455412.738	0.665	1.540	29.38	R	22	4	BRY01
-84.30	2455413.456	0.657	1.534	29.42	R	26	4	LIG01
-81.39	2455416.373	0.625	1.509	29.61	I	22	4	MIL01
-81.34	2455416.419	0.624	1.508	29.63	R	24	4	LIG01
-81.28	2455416.476	0.623	1.508	29.62	R	20	4	BAC01
-80.95	2455416.807	0.620	1.505	29.66	R	34	5	BRY01
-80.39	2455417.369	0.614	1.500	29.69	I	22	4	MIL01
-79.39	2455418.371	0.603	1.492	29.78	I	24	4	MIL01
-78.31	2455419.453	0.591	1.482	29.89	R	22	4	LIG01
-77.37	2455420.391	0.582	1.475	29.97	R	28	4	CRNI1
-73.36	2455424.400	0.541	1.441	30.45	R	23	4	NIC01
-72.36	2455425.395	0.531	1.433	30.59	R	28	4	NIC01
-72.30	2455425.461	0.530	1.432	30.61	R	21	4	LIG01
-70.28	2455427.485	0.510	1.415	30.94	R	26	4	HOR01
-69.39	2455428.370	0.502	1.408	31.09	R	26	4	HOR01
-69.33	2455428.434	0.501	1.407	31.09	R	35	5	CRNI1
-69.30	2455428.455	0.501	1.407	31.09	R	24	4	BAC01
-68.67	2455429.087	0.495	1.402	31.19	R	29	4	FAUL1
-66.38	2455431.382	0.473	1.383	31.64	R	27	4	LIG01
-66.33	2455431.434	0.473	1.383	31.64	R	26	4	CRNI1
-60.46	2455437.295	0.421	1.336	33.00	R	28	4	HOR01
-59.28	2455438.477	0.411	1.327	33.31	Ru	36	5	PRO01
-58.39	2455439.367	0.403	1.321	33.53	R	28	4	NIC01
-58.33	2455439.425	0.403	1.320	33.56	R	34	5	LIG01
-57.45	2455440.308	0.395	1.314	33.79	R	27	4	NIC01
-57.37	2455440.394	0.394	1.313	33.83	R	33	5	BRY01
-57.37	2455440.394	0.394	1.313	33.84	R	31	5	HOR01
-57.28	2455440.482	0.394	1.312	33.86	R	30	5	GAL01
-56.36	2455441.403	0.386	1.305	34.13	R	32	5	LIG01
-55.31	2455442.447	0.378	1.297	34.44	R	42	5	BRY01
-54.29	2455443.474	0.369	1.290	34.75	R	33	5	BRY01
-53.43	2455444.331	0.362	1.283	35.04	R	34	5	HOR01
-51.81	2455445.949	0.350	1.272	35.55	R	35	5	BRY01
-50.95	2455446.808	0.343	1.266	35.84	R	36	5	BRY01
-49.99	2455447.773	0.336	1.259	36.16	R	48	4	BRY01
-49.99	2455447.773	0.336	1.259	36.16	R	52	5	BRY01
-49.89	2455447.874	0.335	1.258	36.21	R	40	5	LIG01
-47.95	2455449.806	0.32	1.244	36.89	R	42	5	BRY01
-47.35	2455450.409	0.316	1.240	37.10	S	39	5	LIG01
-47.05	2455450.711	0.313	1.238	37.21	R	40	5	LIG01
-46.91	2455450.850	0.313	1.238	37.25	R	47	1	BRY01
-46.03	2455451.732	0.306	1.231	37.59	R	41	5	LIG01
-45.87	2455451.893	0.305	1.230	37.64	R	39	5	BRY01
-45.43	2455452.334	0.301	1.227	37.81	R	37	5	BRY01
-44.99	2455452.768	0.298	1.224	37.97	R	41	5	BRY01
-44.18	2455453.577	0.292	1.219	38.27	R	40	5	HOR01
-42.01	2455455.749	0.277	1.205	39.09	R	47	6	LIG01
-40.49	2455457.267	0.267	1.196	39.68	R	43	6	HOR01
-40.43	2455457.330	0.266	1.195	39.70	R	48	6	BRY01
-38.83	2455458.930	0.255	1.185	40.32	R	46	6	BRY01
-37.43	2455460.332	0.246	1.177	40.87	R	40	5	HOR01
-36.39	2455461.371	0.239	1.171	41.27	R	48	6	BRY01
-31.45	2455466.315	0.208	1.144	43.16	R	55	7	BRY01
-30.94	2455466.822	0.205	1.142	43.35	R	61	7	BRY01
-29.94	2455467.818	0.199	1.137	43.72	R	47	6	BRY01
-28.95	2455468.808	0.194	1.132	44.08	R	57	7	BRY01
-27.95	2455469.813	0.188	1.127	44.44	R	54	6	BRY01
-26.89	2455470.872	0.182	1.122	44.82	R	69	8	BRY01
-26.16	2455471.599	0.179	1.119	45.02	R	62	1	BRY01
-26.16	2455471.599	0.179	1.119	45.02	R	61	1	BRY01

(*continued on next page*)

Author's personal copy

Table 2 (*continued*)

Days from T	Julian Date	R (A.U.)	Δ (A.U.)	Phase angle	Phot. band	$Af\rho$ (cm)	err	Observer
-26.16	2455471.599	0.179	1.119	45.02	R	62	1	BRY01
-25.43	2455472.334	0.174	1.116	45.33	R	64	7	LIG01
-21.98	2455475.782	0.158	1.102	46.50	R	74	8	BRY01
-21.28	2455476.483	0.154	1.099	46.74	R	58	7	HOR01
-19.35	2455478.410	0.146	1.092	47.40	R	76	8	BRY01
-18.39	2455479.366	0.143	1.089	47.74	R	87	9	CRNI1
-18.37	2455479.391	0.142	1.089	47.75	R	77	8	BRY01
-17.46	2455480.298	0.139	1.086	48.08	R	85	9	LIG01
-17.41	2455480.350	0.139	1.086	48.10	R	110	11	CRNI1
-17.36	2455480.401	0.139	1.086	48.12	R	94	10	BRY01
-17.18	2455480.577	0.138	1.085	48.18	R	73	8	HAU01
-16.42	2455481.339	0.136	1.083	48.47	R	85	9	CRNI1
-16.26	2455481.501	0.135	1.083	48.54	R	104	10	BRY01
-16.18	2455481.582	0.135	1.082	48.57	R	90	9	HAU01
-15.90	2455481.863	0.134	1.081	48.68	R	98	10	BRY01
-15.46	2455482.303	0.133	1.080	48.86	R	83	9	LIG01
-15.32	2455482.438	0.132	1.080	48.91	R	87	9	CRNI1
-15.32	2455482.438	0.132	1.080	48.91	R	87	9	CRNI1
-15.15	2455482.605	0.132	1.079	48.98	R	88	9	HAU01
-14.99	2455482.771	0.131	1.079	49.05	R	75	8	BRY01
-14.71	2455483.045	0.131	1.078	49.17	R	75	8	FAUL1
-14.03	2455483.732	0.129	1.077	49.46	R	78	8	BRY01
-13.98	2455483.780	0.129	1.076	49.48	R	84	9	LIG01
-13.63	2455484.128	0.128	1.076	49.64	R	96	10	FAUL1
-13.13	2455484.633	0.127	1.074	49.87	R	82	9	CRNI1
-11.78	2455485.982	0.124	1.071	50.53	R	70	8	FAUL1
-8.88	2455488.884	0.121	1.066	52.04	R	91	1	BRY01
-8.88	2455488.884	0.121	1.066	52.04	R	91	1	BRY01
-8.79	2455488.971	0.121	1.066	52.17	R	97	10	CRNI1
-7.98	2455489.780	0.121	1.064	52.65	R	92	1	BRY01
-7.31	2455490.452	0.121	1.064	53.05	R	104	10	LIG01
-6.38	2455491.384	0.121	1.062	53.62	R	115	11	LIG01
-6.10	2455491.659	0.121	1.062	53.79	R	141	13	CRNI1
-6.06	2455491.696	0.121	1.062	53.81	R	125	12	HAU01
-5.87	2455491.891	0.121	1.062	53.93	R	110	11	BRY01
-4.88	2455492.885	0.122	1.061	54.53	R	97	10	BRY01
1.24	2455499.002	0.134	1.059	57.56	R	112	11	FAUl1
1.52	2455499.276	0.135	1.059	57.73	R	100	10	CRNI1
2.13	2455499.893	0.137	1.059	57.94	R	87	9	BRY01
3.09	2455500.850	0.140	1.060	58.22	R	77	8	BRY01
4.15	2455501.912	0.144	1.060	58.47	R	73	8	BRY01
4.33	2455502.088	0.145	1.060	58.50	R	90	9	FAUL1
4.34	2455502.101	0.145	1.060	58.51	R	83	9	FAUL1
5.08	2455502.844	0.147	1.061	58.63	R	83	9	BRY01
5.24	2455503.005	0.148	1.061	58.66	R	85	9	FAUL1
5.36	2455503.123	0.148	1.061	58.67	R	86	9	FAUL1
6.09	2455503.847	0.151	1.062	58.75	R	104	10	BRY01
6.29	2455504.053	0.152	1.062	58.77	R	101	10	FAUL1
6.89	2455504.649	0.154	1.063	58.81	R	109	11	CRNI1
7.17	2455504.932	0.156	1.063	58.82	R	105	10	LIG01
8.18	2455505.938	0.160	1.065	58.82	R	101	10	BRY01
9.22	2455506.977	0.164	1.066	58.77	R	105	10	BRY01
10.08	2455507.841	0.168	1.068	58.68	R	110	11	LIG01
12.09	2455509.845	0.177	1.072	58.35	R	112	11	BRY01
12.15	2455509.913	0.177	1.072	58.33	R	130	12	LIG01
14.12	2455511.879	0.187	1.077	57.84	R	115	11	LIG01
16.12	2455513.881	0.196	1.082	57.18	R	111	11	LIG01
16.15	2455513.914	0.196	1.082	57.17	R	101	10	BRY01
16.94	2455514.700	0.200	1.085	56.88	R	109	11	HAU01
18.21	2455515.969	0.206	1.088	56.36	R	92	9	BRY01
21.22	2455518.982	0.222	1.099	54.98	R	83	9	BRY01
21.22	2455518.982	0.222	1.099	54.98	R	88	9	BRY01
21.22	2455518.982	0.222	1.099	54.98	R	82	9	BRY01
21.22	2455518.982	0.222	1.099	54.98	R	83	9	BRY01
22.20	2455519.955	0.227	1.103	54.49	I	88	9	BRY01
22.24	2455519.998	0.227	1.103	54.47	R	91	9	LIG01
23.23	2455520.99	0.232	1.107	53.95	I	91	9	BRY01
30.22	2455527.978	0.268	1.138	49.86	R	98	10	BRY01
30.22	2455527.978	0.268	1.138	49.86	R	94	10	BRY01
30.23	2455527.986	0.268	1.138	49.86	I	89	9	BRY01
30.23	2455527.986	0.268	1.138	49.86	I	92	9	BRY01
33.16	2455530.917	0.283	1.153	47.98	R	127	12	LIG01
33.16	2455530.917	0.283	1.153	47.98	R	126	12	LIG01
33.22	2455530.981	0.284	1.153	47.94	R	103	10	BRY01
33.22	2455530.981	0.284	1.153	47.94	R	107	11	BRY01

Author's personal copy

Table 2 (*continued*)

Days from T	Julian Date	R (A.U.)	Δ (A.U.)	Phase angle	Phot. band	$Af\rho$ (cm)	err	Observer
33.23	2455530.990	0.284	1.154	47.93	I	99	10	BRY01
33.23	2455530.990	0.284	1.154	47.93	I	89	9	BRY01
38.23	2455535.991	0.310	1.182	44.61	R	83	9	BRY01
38.23	2455535.991	0.310	1.182	44.61	R	79	8	BRY01
38.23	2455535.995	0.310	1.182	44.60	I	60	7	BRY01
38.23	2455535.995	0.310	1.182	44.60	I	75	8	BRY01
39.17	2455536.927	0.315	1.187	43.96	R	110	11	LIG01
39.17	2455536.927	0.315	1.187	43.96	R	110	11	LIG01
39.21	2455536.974	0.315	1.188	43.94	R	114	11	BRY01
40.22	2455537.976	0.320	1.194	43.26	R	92	9	BRY01
40.22	2455537.976	0.320	1.194	43.26	R	97	10	BRY01
40.22	2455537.983	0.321	1.194	43.26	I	94	10	BRY01
40.22	2455537.983	0.321	1.194	43.26	I	90	9	BRY01
43.73	2455541.492	0.339	1.216	40.86	R	117	11	MIL01
45.83	2455543.595	0.351	1.230	39.44	R	106	10	BRY01
47.72	2455545.481	0.362	1.243	38.17	R	111	11	MIL01
67.67	2455565.427	0.487	1.394	26.64	R	91	9	LIG01
78.06	2455575.822	0.568	1.480	23.07	R	75	8	BRY01
78.06	2455575.822	0.568	1.480	23.07	R	72	8	BRY01
78.06	2455575.822	0.568	1.480	23.07	R	77	8	BRY01
79.63	2455577.393	0.581	1.494	22.72	R	78	8	CELA1
80.67	2455578.432	0.590	1.503	22.52	R	88	9	CRNI1
87.64	2455585.401	0.655	1.563	21.71	R	77	8	MIL01
92.57	2455590.330	0.706	1.606	21.64	R	88	9	LIG01
95.61	2455593.373	0.739	1.633	21.75	R	65	7	LIG01
96.63	2455594.394	0.750	1.642	21.81	R	82	9	MIL01
101.62	2455599.382	0.809	1.686	22.23	R	64	7	CELA1
104.55	2455602.311	0.845	1.712	22.54	R	63	7	CRNI1
105.24	2455603.002	0.853	1.718	22.62	R	56	7	AFAM1
107.65	2455605.407	0.884	1.740	22.91	R	66	7	BRY01
126.21	2455623.969	1.151	1.905	25.09	R	59	7	AFAM1
131.54	2455629.300	1.236	1.952	25.55	R	49	6	LIG01
132.57	2455630.330	1.253	1.961	25.63	R	45	6	LIG01
143.55	2455641.309	1.440	2.058	26.21	R	47	6	LIG01
146.60	2455644.358	1.494	2.085	26.29	R	48	6	LIG01
152.54	2455650.300	1.603	2.137	26.35	R	39	5	LIG01
175.59	2455673.346	2.047	2.334	25.46	R	36	5	LIG01
182.20	2455679.959	2.179	2.389	24.92	R	34	5	AFAM1

Columns report: observing time, indicated as days from perihelion and Julian Day, heliocentric and geocentric distances in AU, solar phase angle in degrees, photometric band, $Af\rho$, ± estimated error, Observer code.

Comet 103P/Hartley 2 showed an unprecedented and complex evolution. We observed a rapid variability with large amplitude, indicatively changing the $Af\rho$ by ±50% respect to the average trend. As shown in detail by the EPOXI spacecraft, this observation can be explained by the distribution of active areas on the nucleus.

We gathered that, as seen in Fig. 3 which presents a subset of the measurements around perihelion, the $Af\rho$ shows a high amplitude variations around a fairly constant but high value.

In Fig. 4, we reproduced the same dataset corrected for the solar phase effect (as explained in Section 3) rescaling all the measurements to $\alpha = 0$.

For Comet 103P/Hartley 2 the correction does not change too much the curve shape, except the much higher values, around ~255 cm at maximum, and an outburst peak close to 400 cm.

1998 Data are overplotted (open dots), showing values twice larger than the data obtained at the same time after perihelion during the 2010–2011 apparition, but with a very steep decrease that brings it at about the same level as during this apparition. The flat maximum dominates the top of the curve, while the general trend, ignoring the fast fluctuations, traces out a peak that almost coincides with the perihelion. One can interpret this observation as a flat maximum with local seasonal effects superimposed. The error is apparently larger close to the maximum because it is a relative error and higher values lead to larger error bars.

The plateau around the maximum is very complex, and the variations show apparently a semi-regular periodicity close to 20 days, but that period could be an artifact due to the insufficient sampling of our data.

To perform a more accurate investigation on the brightening/fading rates of Comet 103P/Hartley 2 as it approaches or recedes from the Sun, the $Af\rho$ quantity has been analyzed vs. the heliocentric distance (Fig. 5).

The asymmetry of the curve and of the ascending and descending branches are enhanced and we can better see the fast evolution for R < 1.6 AU. A simple constant power law of the heliocentric distance R^a type cannot describe this behavior, where a is the coefficient that determines how fast the comet brightens approaching to the Sun. For 103P/Hartley 2 the log-slope increased with time approaching perihelion. The average slope is close to $a \approx -4$, but a was close to -0.8 ± 0.5 in the early period, at an heliocentric distance $1.6 < R < 1.9$ AU (estimate based on a few data only), and -3.66 ± 0.14 in the range of $1.01 < R < 1.70$ AU.

It apparently approaches to a value as high as -8 by the end of the ascending branch, just before maximum, but in that period, outbursts and the high variability can have affected the results (Fig. 6).

The descending branch again shows some irregularities, but the average behavior is in fairly good agreement with a constant power law, with $a = -1.66 \pm 0.13$ in the range of $1.4 < R < 2.4$ AU (Fig. 7).

At first glance one could think that the irregularities were due to some uncorrected observational errors or to problems related to relatively crowded starfields, but observing the high degree of variability toward perihelion we reconsidered the possibility that the scattering was related to real variations. We found a small outburst occurred on August 10 (see Section 6).

Author's personal copy

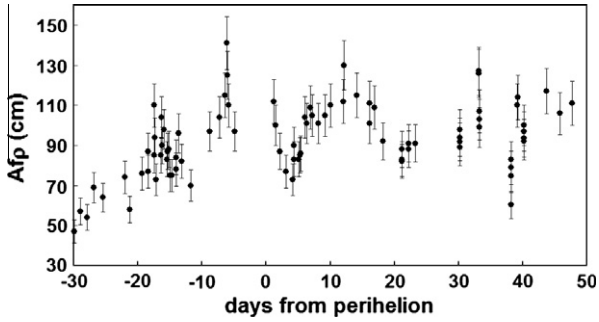

Fig. 3. A subset of $Af\rho$ quantity data around the maximum (−30 to +50 days from perihelion) shows high amplitude variations around an average value close to 100 cm. The data are not corrected for solar phase angle.

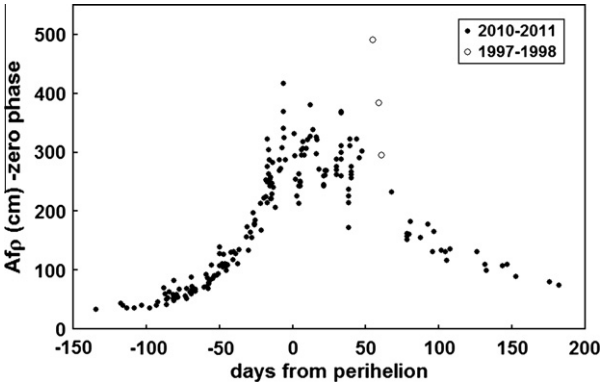

Fig. 4. $Af\rho$ quantity (cm) referred to the R band and corrected for a zero phase angle. The same as in Fig. 2 but after correction to solar phase. Only R band data are plotted. Dots refer to the 2010–2011 apparition, open circles to the 1997–1998 one. Error bars are omitted for better perspicuity.

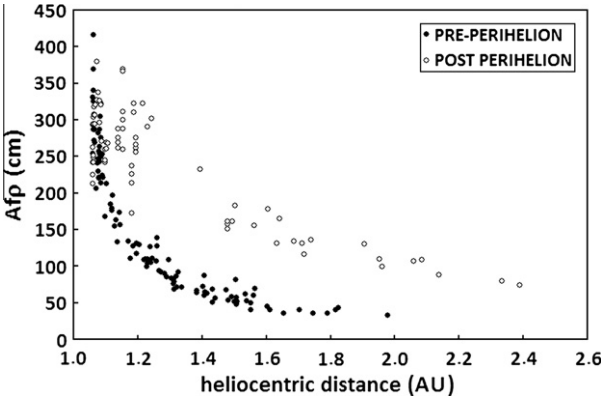

Fig. 5. The $Af\rho$ quantity (cm) referred to the R band and corrected for a zero phase angle is plotted vs. the heliocentric distance. Dots refer to the 2010–2011 pre perihelion data, open circles to the post perihelion ones. The difference in the brightening and fading rates is enhanced. Error bars are omitted for clarity.

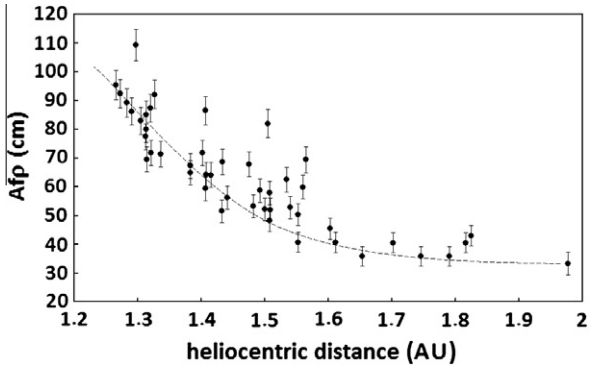

Fig. 6. A close up of the ascending branch shows a super exponential increment of the $Af\rho$ quantity that cannot be represented by a constant power law. At R > 1.6 AU $Af\rho$ apparently follows an $R^{-0.8}$ trend (estimate based on few data), but at an heliocentric distance smaller than 1.6 AU it rapidly increases to R^{-4}, or even above. The dashed line is only indicative.

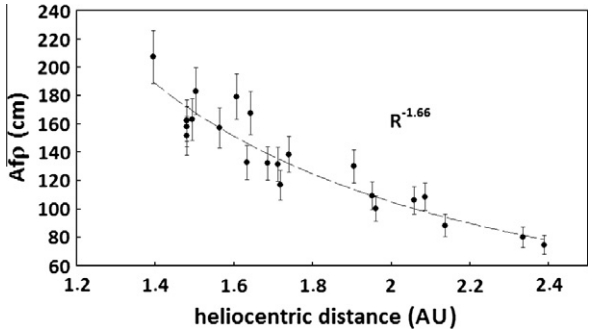

Fig. 7. The descending branch starts about 50 days after perihelion and shows a more regular trend in average with $Af\rho$ following an $R^{-1.6}$ power law.

Table 3
Observed outbursts.

Date (2010)	J.D.	Apparent $Af\rho$ peak	Apparent $Af\rho$ increment	Figure
August 10	2455417.369	31 cm (I band) ± 3	50%	8a
October 9	2455479.366	113 cm (R) ± 12	40%	8b
October 10	2455480.350	146 cm (R) ± 13	70%	8c
October 11	2455481.339	107 cm (R) ± 16	40%	8d
October 12	2455482.438	114 cm (R) ± 17	40%	8e
October 13	2455482.605	110 cm (R) ± 10	40%	
October 14	2455483.779	144 cm (R) ± 12	80%	8f
October 19	2455488.971	110 cm (R) ± 12	Small-suspected	8g
October 22	2455491.658	160 cm (R) ± 18	75%	8h
October 29	2455499.002	200 cm (R) ± 16	250%	8i
November 2	2455503.004	99 cm (R) ± 8	Small-suspected	8j
November 4	2455504.648	123 cm (R) ± 15	40%	8k

Columns report: Month and day, Julian day, apparent $Af\rho$ peak value, apparent % increase, reference figure.

An interesting coincidence is that the ascending branch, perhaps accompanied by a short term variability, starts nearly at the same time when the rotation period of the nucleus was slowing down (Meech et al., 2011; Drahus et al., 2011). The rotation period in April–May 2009 was measured to be 16.4 ± 2 h. The same period was reported in August 2010 but toward October it increased to 18.1 ± 0.3 h and in early November it was confirmed at 18.4 ± 0.3 h. In the second half of November it was nearly 19 h (A'Hearn et al., 2011; Meech et al., 2011; Samarasinha et al., 2011).

This scenario suggests that the increasing activity of the nucleus in August 2010 may have been related to the changing rotation rate; also accompanied by short term variability, possibly related to seasonal effects and the exposition of the more active areas to solar radiation.

The maximum phase was characterized by strong fast variations observed from 2010 early October. The variations proved to be very fast but unluckily, the sampling of our observations was not enough to resolve clearly this short term periodicity.

Author's personal copy

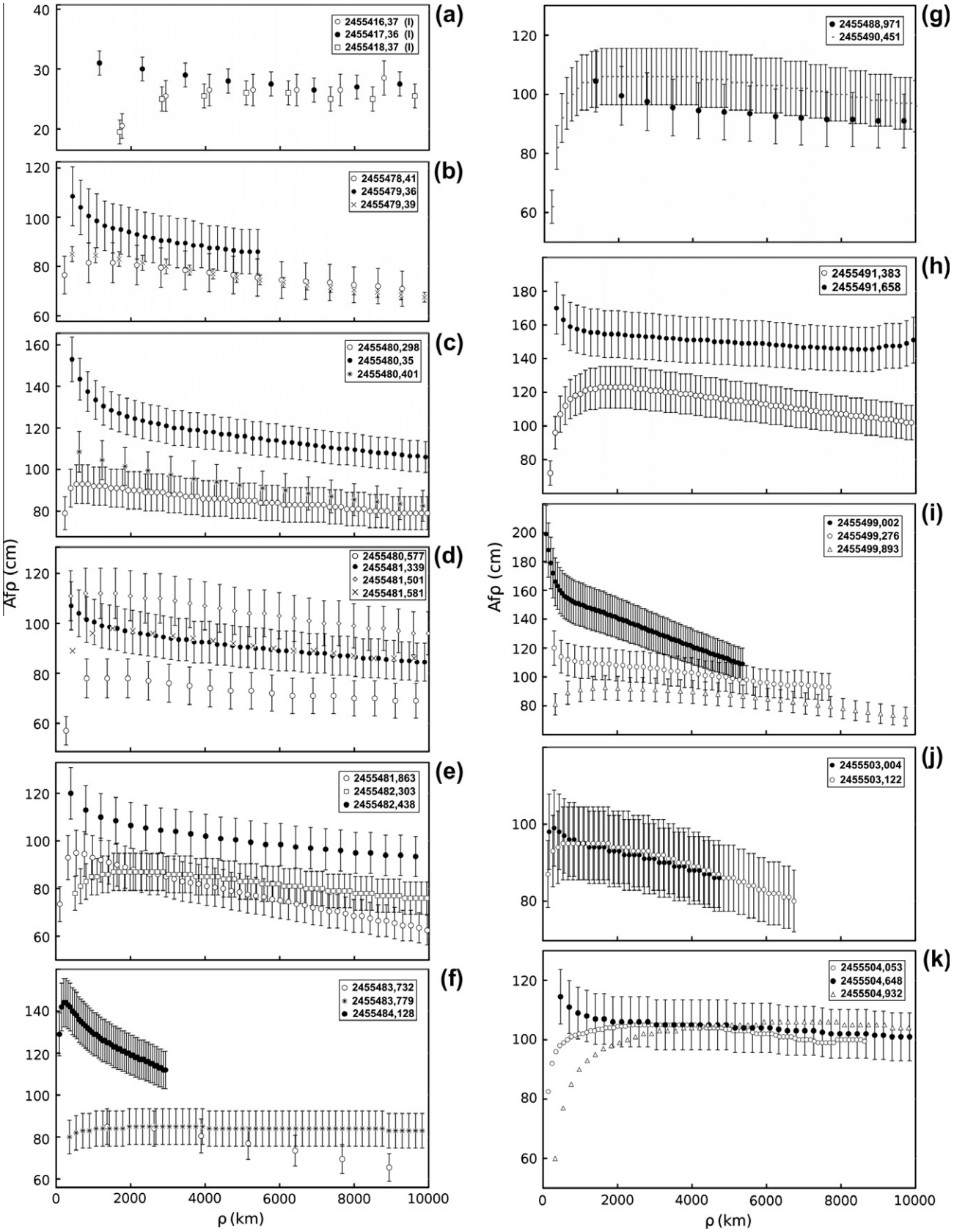

Fig. 8. The small outbursts detected by the average slope $Af\rho$ vs. ρ analysis. During the events unusual high $Af\rho$ values are observed at small ρ. Data of the closest available observing runs with a normal profile are reported as comparison. Except where indicated all observations are in R band (details are summarized in Table 3).

Author's personal copy

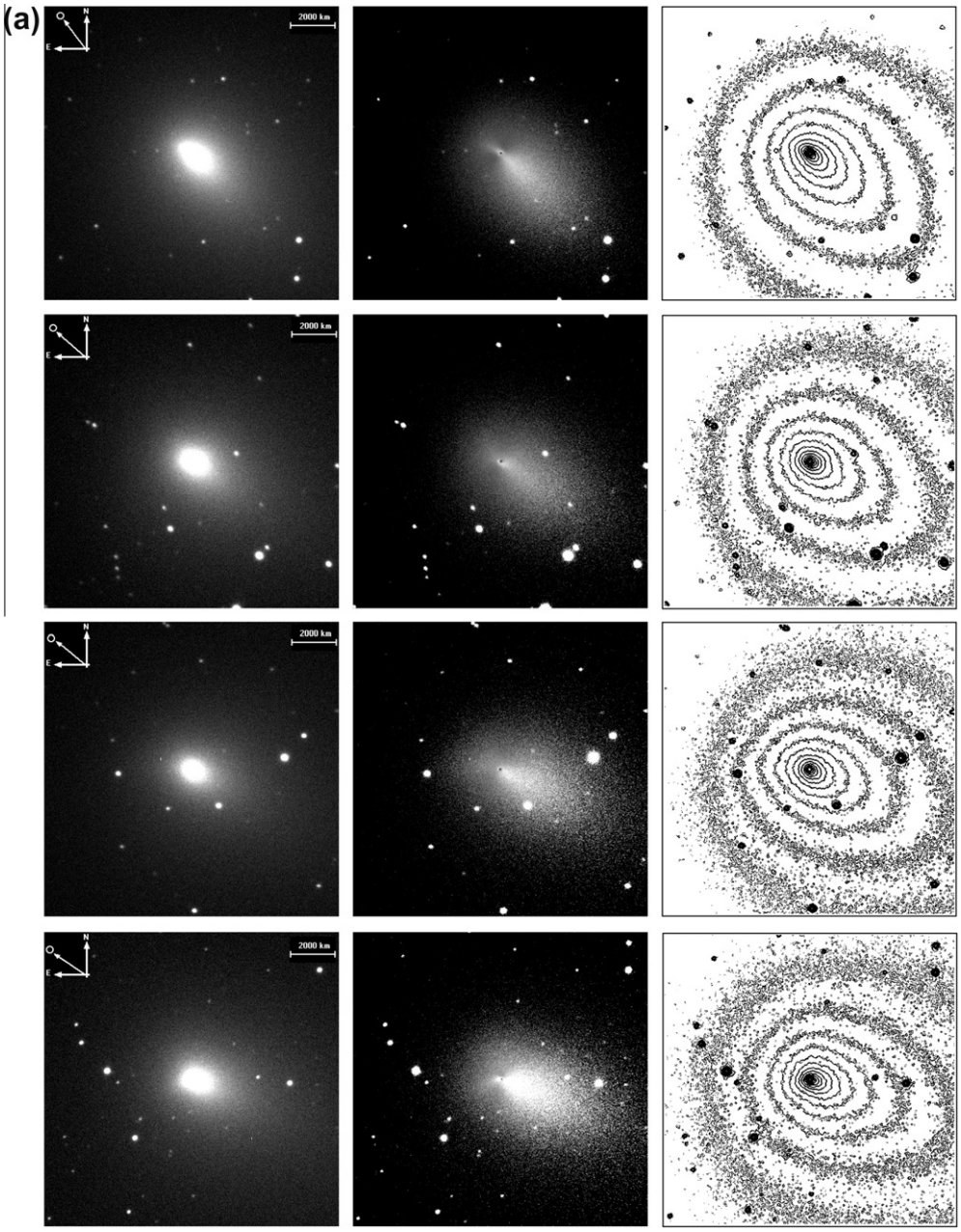

Fig. 9. (a and b) R band Faulkes Telescope North images of 103P/Hartley 2, obtained in October and November 2010. Columns show the original images, RM processed images, and isophotes of RM processed images, respectively. The divergence from the 1/rho model and the changing in the brightness distribution reflects the high variability of the nucleus activity. Different rows show images from: (a) 2010 October 11.57 UT, October 14.63 UT, October 15.56 UT, October 16.51 UT. (b) 2010 October 29.50 UT, November 1.60 UT, November 10.62 UT, November 15.50 UT.

6. The outbursts activity

The comet was best observable around the perihelion and the encounter. That time, the strong variability of matter production was also observed by the spacecraft. (A' Hearn et al., 2011).

The variability was related to small outbursts that were continuously monitored by the EPOXI spacecraft during the flyby, which was detected also by other authors (Tozzi et al., 2012) with groundbased observations over a longer period.

We seeked the signs of small outburts in the log-slope of $Af\rho$. This analysis allows to explore the average coma profile, that in the case of a comet with a coma gradient according to $1/\rho$, should give a constant $Af\rho$ value for a wide range of distances from the nucleus. In a normal status we usually observe a nearly constant value, that corresponds to a steady state activity, with no radiation pressure, or a fading trend with a slope depending from how much the gradient diverges from $1/\rho$. The analysis can usually be performed starting from a minimum distance from the nucleus that excludes smaller ρ in the range affected by seeing, thus avoiding an underestimation of the $Af\rho$. Despite this $Af\rho$ problem, the region affected by seeing can still tells us some useful information when it displays unusually high values. Excluding some instrumental effects (e.g. the accidental superposition of a foreground star) this usually indicates the occurrence of an outburst.

Our $Af\rho$ vs. ρ analysis allowed to identify several periods of intense activity or outbursts listed in Table 3 and plotted in Fig. 8.

Please note that the increments, here and after, are estimated comparing the available plots for nearby data profiles. Calibration

Author's personal copy

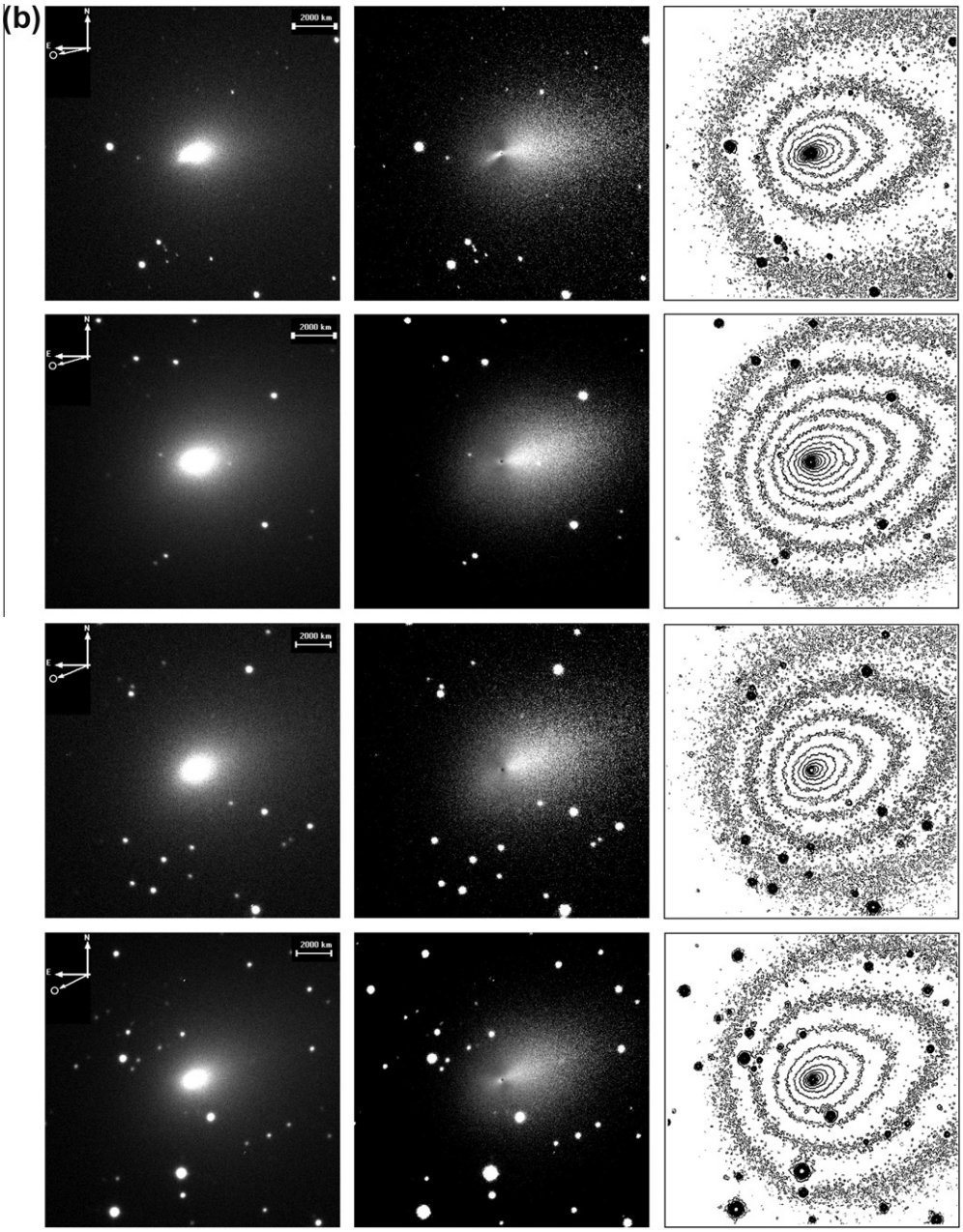

Fig. 9. (*continued*)

Fig. 10. Comet 103P/Hartley 2 observed with the 36-cm. f/6.7 S-C telescope of the Črni Vrh Observatory on 1998 February 21.827 UT. The morphology is comparable with that shown in the 2010–2011 apparition. Images are processed as in Fig. 9a and b.

Author's personal copy

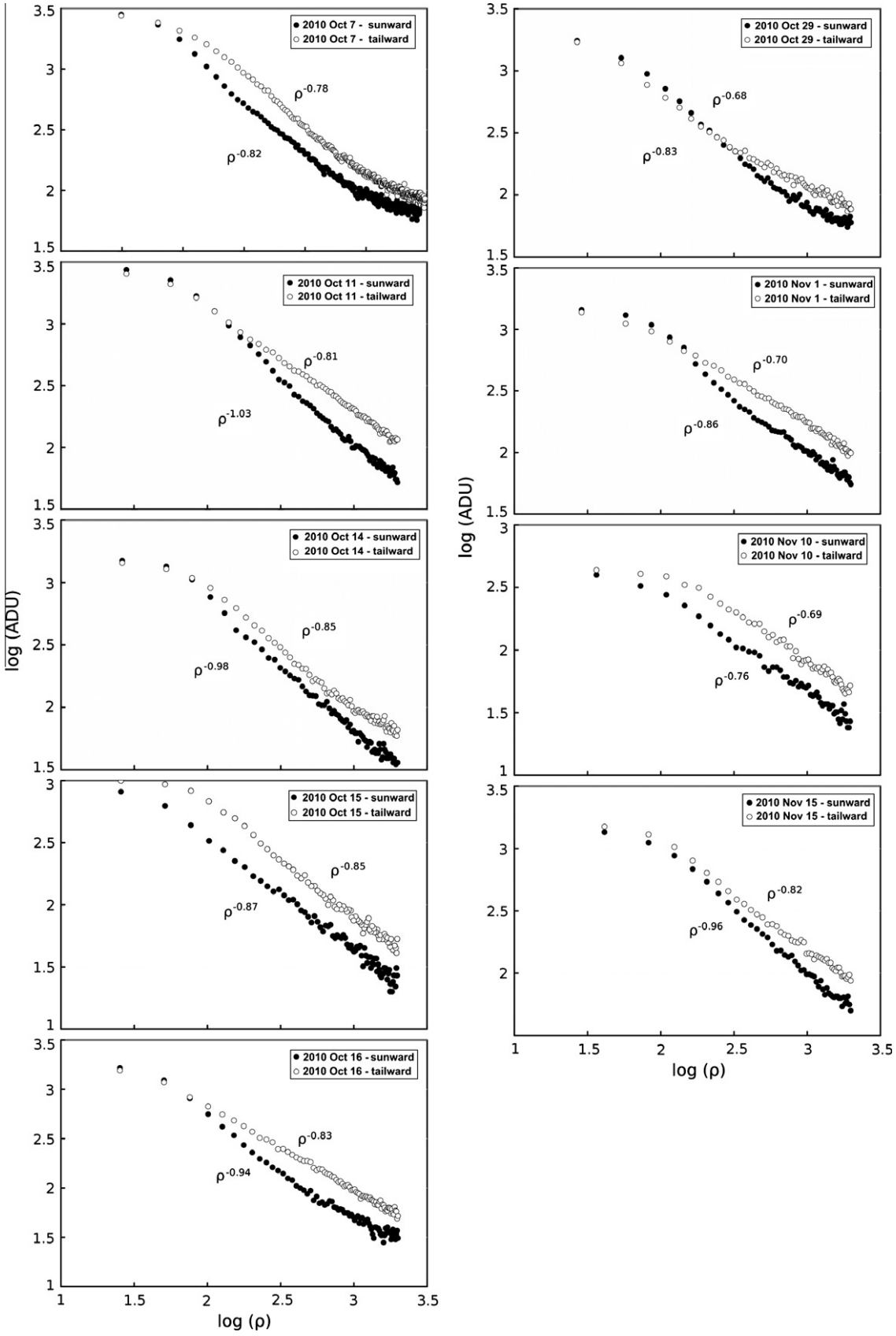

Fig. 11. The coma gradient analysis performed on Faulkes Telescope North images shows consistent daily and local variations. The profile has been analyzed within 2000 km from the nucleus by means of log (ADU) (arbitrary unit) and the projected distance from the nucleus (ρ) in km.

Author's personal copy

problems related to the use of different reference stars, and small residual instrumental effects, cause a shifts in the average $Af\rho$ values in some plots. This limits the possibility to trace the evolution of the $Af\rho$ vs. ρ profile related to the motion of the dust. But these variations are compatible with the average observational error and do not affect the analysis where deviations form a regular profile at small ρ can indicate the occurrence of small outbursts. In our case some events are evident but others are close to our detection limit. Despite these approximations, the relative amplitude of the outbursts are comparable with the flux variations observed by the EPOXI spacecraft during the flyby (A' Hearn et al., 2011).

7. Imaging

To complete the photometric analysis, it is interesting to consider the imaging too. In particular, it is useful to perform an image processing with a proper tool based on an $1/\rho$ gradient trend.

This is generally important for photometry, and particularly for $Af\rho$ analysis as in a coma displaying an $1/\rho$ gradient the value is constant and independent from the size of the measuring window and from ρ.

This condition is the consequence of a theoretical steady state coma where dust expands at constant speed in isotropic mode (Massonne, 1994; Lamy, 1986). Comparing a real coma to a theoretical model with an $1/\rho$ gradient gives information on the spatial distribution of dust.

We applied an image processing package named Radial Model (RM) specifically developed as a plug-in for the Astroart (MSB) software (plugin freely downloadable at http://cara.uai.it/soft_list). This kind of process normalizes the coma to an $1/\rho$ brightness distribution (Grun et al., 1986; Bonev and Jockers, 2002) enhancing the deviations with respect to this model. In Figs. 9 and 10, we plot representative images from the 2010 to 2011 apparition (Faulkes Telescope North) and from 1997 to 1998 (Črni Vrh Observatory). Isophotes refer to the $1/\rho$ normalized images.

The normalized images show a constant tailward asymmetry and a steeper sunward slope with strong variations depending on the rapid changes in the activity. This variability was also reported by Lara (Lara et al., 2011).

This aspect is better resolved around perihelion when finer resolution images have been taken, but it is still well detectable elsewhere in the active state. This asymmetry is also evident in the images taken in 1998, suggesting it is a recurrent characteristic of this comet.

The relative brightness tailward peak can perhaps be related to the sublimation and fragmentation of the large size icy particles observed in situ by the EPOXI spacecraft (A' Hearn et al., 2011; Combi et al., 2011).

The tailward peak could be related to gas emissions but also to small dust grains ejected at very small speed from the icy particles and accelerated in the antisolar direction by radiation pressure.

To better analyze the coma profile along the direction of the projected radius vector and the analysis of the sunward and tailward gradients, a check has been made on several images. Because of the favorable image scale (km/arcsec) and of the particular variable morphology and asymmetry, best useful results have been achieved on the Faulkes Telescope North images. The average gradient, measured within 2000 km from the nucleus is shown in Fig. 11. On an average the gradient is from $\rho^{-0.7}$ to $\rho^{-1.0}$, with local variations both depending on the changing activity of the nucleus and on the range of distances used for calculations.

8. Summary

The 103P/Hartley 2 observing campaign allowed an extended monitoring of the comet during the 2010/2011 apparition, from June 2010 to April 2011. After an apparent steady state (observed from −135 to −100 days before perihelion) close to $\sim R^{-1}$ the behavior of the comet was characterized by a super-exponentially rising ascending branch from −100 days up to −15 days before perihelion, with an average growing rate close to $\sim R^{-4}$ but reaching apparently values as high as −8 before maximum.

It was followed by a nearly flat maximum lasting from 15 to +50 days from perihelion, with an apparent average $Af\rho$ quantity close to 100 cm (about 255 cm if corrected to a zero phase angle), but characterized by fast variations between $Af\rho$ 60–140 cm. The apparently flat maximum was centered about at 20 days after perihelion. The descending branch was monitored until +182 days after perihelion. The solar conjunction unluckily did not allow us to observe the comet for a longer time. The fading was exponential-like with an average rate of $R^{-1.7}$.

The strong short term variability was a relevant characteristic of this comet. We were seeking for signs of small outbursts in the log-slopes, revealing 10 certain and two suspected events, with an $Af\rho$ quantity increase ranging between 40% and 250% in the smaller photometric measuring aperture (ρ < 1000 km).

A comparison with three data points from the 1997/1998 apparition shows, on an average, a bit higher $Af\rho$ values and the same short term variability.

The comet morphology displays noticeable changes and often a pronounced asymmetry. Image processing reveals, as a general trend, a relative tailward brightening excess, possibly related to the large icy fragments ejection observed in situ by the EPOXI spacecraft. This asymmetry is evident also in the 1998 images and is apparently a recurrent characteristic of this comet.

The average sunward and tailward coma gradient measured along the projected radius vector shows daily variations and also a complex trend. The average gradient measured within 2000 km from the nucleus is around −0.8 –1.0 generally with a slightly steeper sunward gradient.

Acknowledgments

We thank all people who contributed and supported the development of the CARA Project, and in particular M. Fulle, G.P. Tozzi and M. A'Hearn for encouraging us in the Project.

We thanks also Stefano Sello for his additional tentative to look for periodicities in our data.

The Faulkes Telescope North and Tzec Maun Foundation, are acknowledged for having allowed us to the use their remotely controlled telescopes. The work at Ondřejov was supported by the Grant Agency of the Czech Republic, Grant 205/09/1107. GyMSz was supported by Hungarian OTKA Grants K-104607, MB08C 81013, a 'Lendulet' Programme and a Bolyai Research Fellowship of the Hungarian Academy of Sciences (GyMSz). We thanks the anonymous Reviewers for their help in improving the paper.

Appendix A. Supplementary material

Supplementary data associated with this article can be found, in the online version, at http://dx.doi.org/10.1016/j.icarus.2012.09.004. These data include Google maps of the most important areas described in this article.

References

A'Hearn, M.F., Schleicher, D.G., Millis, R.L., Feldman, P.D., Thompson, D.T., 1984. Comet Bowell 1980b. Astron. J. 89, 579–591.
A'Hearn, M.F. et al., 2005. Deep impact: Excavating Comet Tempel 1. Science 310, 258–264.
A' Hearn, M.F. et al., 2011. EPOXI at Comet Hartley 2. Science 332, 1396–1400.
Bessel, M.S., 1990. UBVRI Passbands. Publ. Astron. Soc. Pacific 102, 1181–1199.

Author's personal copy

Bonev, T., Jockers, K., 2002. Spatial distribution of the dust color in Comet 2000 WM1(LINEAR) ACM 2002. In: Barbara Warmbein (Ed.), International Conference, 29 July–2 August 2002, Berlin. Germany, ESA SP-500. ESA Publications Division, Noordwijk, Netherlands, pp. 587–591. ISBN:92-9092-810-7.

Colangeli, L. et al., 1999. Infrared spectral observations of Comet 103P/Hartley 2 by ISOPHOT. Astron. Astrophys. 343, L87–L90.

Combi, M.R., Bertaux, J.L., Quémerais, E., Ferron, S., Mäkinen, J.T.T., 2011. Water production by Comet 103P/Hartley2 observed with the SWAN instrument on the SOHO spacecraft. Astrophys. J. 743, L6–L11.

Crovisier, J., Brooke, T.Y., Leech, K., et al., 2004. The composition of ices in Comet C/1995 O1 (Hale-Bopp) from radio spectroscopy. Further results and upper limits on undetected species. Astron. Astrophys. 418, 1141–1157.

Drahus, M., Jewitt, D., Guilbert-Lepoutre, A., Waniak, W., Hoge, J., Lis, D.C., Yoshida, H., Peng, R., Sievers, A., 2011. Rotation of Comet 103P/Hartley 2 from spectroscopy at 1 mm. Astrophys. J. 734, L2–L7.

Fulle, M., Mikuz, H., Bosio, S., 1997. Dust environment of Comet Hyakutake (1996 B2). Astron. Astrophys. 324, 1197–1205.

Fulle, M., Barbieri, C., Cremonese, G., et al., 2004. The dust environment of Comet 67P/Churyumov-Gerasimenko. Astron. Astrophys. 422, 357–368.

Fulle, M., Barbieri, C., Cremonese, G., et al., 2010. Comet 67P/Churyumov–Gerasimenko: The GIADA dust environment model of the Rosetta Mission target. Astron. Astrophys. 522, A63.

Grosussin, O., Lamy, P., Jorda, L., et al., 2004. The nuclei of Comets 126P/IRAS and 103P/Hartley 2. Astron. Astrophys. 419, 375–383.

Grun, E., Graser, U., Kohoutek, L., et al., 1986. Structures in the coma of Comet Hally. Nature 321, 144–147.

Hambly, N.C., Irwin, M.J., MacGillivray, H.T., 2001. The SuperCOSMOS Sky Survey – II. Image detection, parametrization, classification and photometry. Mon. Not. R. Astron. Soc. 326, 1295–1314.

Hardorph, J., 1978. The Sun among the stars I: A search for solar spectral analogs. Astron. Astrophys. 63, 383–390.

Hartogh, P. et al., 2011. Ocean-like water in the Jupiter-family Comet 103P/Hartley 2. Nature 478, 218–220.

Lamy, P.L., 1986. Cometary dust-observational evidences and properties. In: Asteroids, Comets, Meteors II. Uppsala Univ. Press, Uppsala, pp. 373–388.

Lara, L.M., Lin, Z.-Y., Meech, K., 2011. Comet 103P/Hartley 2 at perihelion: Gas and dust activity. Astron. Astrophys. 532, 1–11.

Lisse, C.M., Fernandez, Y.R., Reach, W.T., et al., 2009. Spitzer space telescope observations of the nucleus of Comet 103P/Hartley 2. Publ. Astron. Soc. Pacific 121, 968–975.

Massonne, L., 1994. The modelling of cometary dust features. Comet Halley: Investigations, Results, Interpretations, vol. 2. J. Whiley & Sons Ed., England, pp. 65–78.

Meech, K.J., 2011. EPOXI: Comet 103P/Hartley 2 observations from a worldwide campaign. Astrophys. J. 734(L1), 1–9.

Milani, G.A., Szabó, Gy.M., Sostero, G., Trabatti, R., Ligustri, R., Nicolini, M., Facchini, M., Tirelli, D., Carosati, D., Vinante, C., Higgins, D., 2007. Photometry of Comet 9P/Tempel 1 during the 2004/2005 approach of the deep impact module impact. Icarus 187, 276–284.

Nakano, S., Green, D.W.E., 2009. 2009/2010 Comet Handbook. ICQ Special Issue. SAO.

Nakano, S., Green, D.W.E., 2011. 2011/2012 Comet Habdbook. ICQ Special Issue. SAO.

Samarasinha, N.H., Mueller, B.E.A., A'Hearn, M.F.A., Farnham, T.L., Gersch, A., 2011. Rotation of Comet 103P/Hartley 2 from structures in the coma. Astrophys. J. 734, L3–L9.

Schleicher, D.G., 2007. Deep impact's target Comet P/Tempel 1 at multiple apparitions: Seasonal and secular variations in gas and dust production. Icarus 191, 322–338.

Schleicher, D.G., Bair, A.N., 2011. The composition of the interior of Comet 73P/Schwassmann–Wachmann 3: Results from narrowband photometry of multiple components. Astron. J. 141, 177–196.

Schleicher, D.G., Millis, R.L., Birch, P.V., 1998. Narrowband photometry of Comet P/Halley: Variation with heliocentric distance, season, and solar phase angle. Icarus 132, 397–417.

Snodgrass, C., Meech, K., Hainauts, O., 2010. The nucleus of 103P/Hartley 2, target of the EPOXI mission. Astron. Astrophys. 516, L9–L12.

Szabó, Gy.M., Kiss, L.L., Sàrneczky, K., Szilàdi, K., 2002. Spectrophotometry and structural analysis of 5 comets. Astron. Astrophys. 384, 702–710.

Szabó, G.M., Milani, G., Vinante, C., Ligustri, R., Sostero, G., Trabatti, R., 2010. Observations of bright comets in CARA archives I: Years 2002–2006. Earth Moon Planets 107, 253–265.

Tozzi, G.P. et al., 2012. Activity of Comet 103P/Hartley 2 at the time of the EPOXI mission fly-by. Icarus 222, 766–773.